Shuttle-Mir Science Program Phase 1A Research Postflight Science Report

March 1998

National Aeronautics
and Space Administration

Lyndon B. Johnson Space Center
Houston, TX

Contents

INTRODUCTION v

SECTION 1: METABOLISM REPORTS

2.1.1 Fluid and Electrolyte Homeostasis, Dynamics of Calcium Metabolism and Bone Tissue, Red Blood Cell Mass and Survival (Mir 18 Final Science Report) 1-3

2.1.3 Renal Stone Risk Assessment During Long-Duration Space Flight (Mir 18 Final Science Report) 1-9

2.2.3 Metabolic Response to Exercise (Mir 18 Final Science Report) 1-19

2.2.4 Metabolism of Red Blood Cells (Mir 18 Final Science Report) 1-21

2.3.1 Physiologic Alterations and Pharmacokinetic Changes During Space Flight (Mir 18 Final Science Report) 1-25

2.4.2 Assessment of Humoral Immune Function During Long-Duration Space Flight (STS-71 Final Science Report) 1-35

2.4.3 Reactivation of Latent Viral Infections in the Mir Crew (Mir 18 Final Science Report) 1-41

2.4.3 Reactivation of Latent Viral Infections in the Mir Crew (Mir 19 Final Science Report) 1-49

2.4.4 Phenotypic and Functional Analysis of Peripheral Mononuclear Cells During Long-Duration Space Flight (STS-71 Final Science Report) 1-55

SECTION 2: CARDIOVASCULAR AND CARDIOPULMONARY REPORTS 2-1

3.1.1 Studies of Orthostatic Intolerance with the Use of Lower Body Negative Pressure (LBNP) (Mir 18 Final Science Report) 2-3

3.1.2 Studies of Mechanisms Underlying Orthostatic Intolerance Using Ambulatory Monitoring, Baroreflex Testing and the Valsalva Maneuver (STS-71 Final Science Report) 2-11

3.2.1 Aerobic Capacity Using Graded Bicycle Ergometry (Mir 18 Final Science Report) 2-19

3.2.2 Evaluation of Thermoregulation During Long-Duration Space Flight (Mir 18 Final Science Report) 2-31

3.3.1 Physiological Responses to Descent on the Space Shuttle (STS-71 Final Science Report) 2-43

SECTION 3: NEUROSCIENCE REPORTS 3-1

4.1.1 Skeletal Muscle Performance and Characteristics (Mir 18 Final Science Report) 3-3

4.1.2 Morphological, Histochemical, and Ultrastructural Characteristics of Skeletal Muscle (Mir 18 Final Science Report) 3-13

4.2.1 Eye-Head Coordination During Target Acquisition (Mir 18/19 Final Science Report) 3-25

4.2.4 Biomechanics of Movement During Locomotion (Mir 18 Final Science Report) 3-53

4.2.4 Biomechanics of Movement During Locomotion (Mir 19 Final Science Report) 3-69

4.2.4 Alterations in Postural Equilibrium Control Associated With Long-Duration Space Flight (Mir 18 Final Science Report) 3-79

4.2.4 Alterations in Postural Equilibrium Control Associated With Long-Duration Space Flight (Mir 19 Final Science Report) 3-91

4.2.4 Anticipatory Postural Activity (POSA) (Mir 18 Final Science Report) 3-103

4.2.4 Anticipatory Postural Activity (POSA) (Mir 19 Final Science Report) 3-109

SECTION 4: HYGIENE, SANITATION AND RADIATION REPORTS 4-1

5.1 Microbiological Investigations of the Mir Space Station and Flight Crew (Mir 18 Final Science Report)..... 4-3
5.1 Microbiological Investigations of the Mir Space Station and Flight Crew (Mir 19 Final Science Report)..... 4-61
5.2.1 Inflight Radiation Measurements (Mir 18 Final Science Report)..... 4-93
5.2.1 Inflight Radiation Measurements (Mir 19 Final Science Report)..... 4-101
5.2.6 Cytogenetic Effects of Space Radiation in Human Lymphocytes (Mir 18 Final Science Report)..... 4-103
5.3 Toxicological Assessment of Air Contaminants (Mir 18 Final Science Report)..... 4-111
5.3 Toxicological Assessment of Air Contaminants (Mir 19 Final Science Report)..... 4-125
5.3 Trace Chemical Contamination: Water Quality (Mir 18 Final Science Report)..... 4-153
5.3 Trace Chemical Contamination: Water Quality (Mir 19 Final Science Report)..... 4-167

SECTION 5: BEHAVIOR AND PERFORMANCE REPORTS..... 5-1

6.2.2 The Effectiveness of Manual Control During Simulation of Flight Tasks (Pilot) (Mir 18 Final Science Report)..... 5-3

SECTION 6: FUNDAMENTAL BIOLOGY REPORTS..... 6-1

7.1.1 Incubator Experiment (Mir 18/19 Final Science Report)..... 6-3
7.1.2 Greenhouse - Integrated Plant Experiments on Mir (Mir 19 Final Science Report)..... 6-7

SECTION 7: MICROGRAVITY..... 7-1

8.1.1 Space Acceleration Measurement System (SAMS) on Mir (Mir 19 Final Science Report)..... 7-3
8.1.3 Protein Crystal Growth (PCG)/GN2 Dewar Experiment (Mir 19 Final Science Report)..... 7-7

Introduction

The Shuttle-Mir Science Program, also known as the Phase 1A program, was developed as a result of a joint agreement between the United States and the Russian Federation which initiated a cooperative human space flight program. The program consisted of two long duration missions, Mir 18 and Mir 19, and one Shuttle docking mission, Spacelab-Mir (SL-M) STS-71.

The Mir 18 mission began with the launch of the Soyuz TM21 on March 14, 1995, carrying two Russian cosmonauts, Mission Commander Lieutenant Colonel Vladimir N. Dezhurov and Flight Engineer Gennady M. Strekalov, Ph.D., and U.S. Astronaut, Mission Specialist Norman E. Thagard, M.D. The Soyuz TM21 docked with the Mir on March 16, 1995. After a 116 day stay in space, most of it on the Russian Space Station Mir, the Mir 18 crew landed at Kennedy Space Center on July 7, 1995. The STS-71 crew consisted of Commander Captain Robert L. "Hoot" Gibson, Pilot Lieutenant Colonel Charles J. Precourt, Mission Specialist Ellen S. Baker, M.D., Mission Specialist Gregory J. Harbaugh and Mission Specialist Bonnie J. Dunbar, Ph.D. The SL-M mission also provided return transportation for the Mir 18 crew and transportation for the Mir 19 crew to the Mir.

The Mir 19 mission continued the joint science program and began with the launch of U.S. Space Shuttle Atlantis carrying two Russian cosmonauts, Mission Commander Colonel Anatoly Y. Solovyev and Flight Engineer Nikolai M. Budarin, to the space station Mir. Mir 19 was concluded on September 11, 1995, with the landing of Soyuz TM21 in Russia.

The Shuttle-Mir science program used the U.S. Space Shuttle and the Russian Space Station Mir capabilities to conduct joint research activities in space. Seven research areas encompassing 28 investigations were conducted on Mir and/or the Shuttle. The overall objectives of the Shuttle-Mir missions were to obtain engineering and operational experience in conducting research on an orbital space station; to conduct specific investigations in medical support, life sciences, fundamental biology, microgravity sciences, Earth observations, and life support technology; and to characterize the environment relative to microgravity and life sciences research on Mir to better understand past and future investigations. Included in this report are the final science reports from the investigations performed on Mir 18, STS-71, and/or Mir 19.

Section 4: Hygiene, Sanitation and Radiation Reports

Exp#	Experiment Title	Page
5.1	**Microbiological Investigations of the Mir Space Station and Flight Crew (Mir 18 Final Science Report)**	4-3
	U.S. Principal Investigator: **DUANE L. PIERSON, Ph.D.,** NASA/Johnson Space Center *Russian Principal Investigator:* **ALEKSANDR N. VIKTOROV, M.D.,** Institute of Biomedical Problems	
5.1	**Microbiological Investigations of the Mir Space Station and Flight Crew (Mir 19 Final Science Report)**	4-61
	U.S. Principal Investigator: **DUANE L. PIERSON, Ph.D.,** NASA/Johnson Space Center *Russian Principal Investigator:* **ALEKSANDR N. VIKTOROV, M.D.,** Institute of Biomedical Problems	
5.2.1	**Inflight Radiation Measurements (Mir 18 Final Science Report)**	4-93
	U.S. Principal Investigator: **GAUTAM D. BADHWAR, Ph.D.,** NASA/Johnson Space Center *Russian Principal Investigator:* **V. M. PETROV,** Institute of Biomedical Problems	
5.2.1	**Inflight Radiation Measurements (Mir 19 Final Science Report)**	4-101
	U.S. Principal Investigator: **GAUTAM D. BADHWAR, Ph.D.,** NASA/Johnson Space Center *Russian Principal Investigator:* **V. M. PETROV,** Institute of Biomedical Problems	
5.2.6	**Cytogenetic Effects of Space Radiation in Human Lymphocytes (Mir 18 Final Science Report)**	4-103
	U.S. Principal Investigator: **TRACY CHUI-HSU YANG, Ph.D.,** NASA/Johnson Space Center *Russian Principal Investigator:* BORIS FEDORENKO, M.D., Institute of Biomedical Problems	
5.3	**Toxicological Assessment of Air Contaminants (Mir 18 Final Science Report)**	4-111
	U.S. Principal Investigator: **JOHN T. JAMES,** NASA/Johnson Space Center	
5.3	**Toxicological Assessment of Air Contaminants (Mir 19 Final Science Report)**	4-125
	U.S. Principal Investigator: **JOHN T. JAMES,** NASA/Johnson Space Center	
5.3	**Trace Chemical Contamination: Water Quality (Mir 18 Final Science Report)**	4-153
	U.S. Principal Investigator: **RICHARD W. SAUER, P.E.,** NASA/Johnson Space Center *Russian Principal Investigator:* YURI SINYAK, M.D., Institute of Biomedical Problems	
5.3	**Trace Chemical Contamination: Water Quality (Mir 19 Final Science Report)**	4-167
	U.S. Principal Investigator: **RICHARD W. SAUER, P.E.,** NASA/Johnson Space Center *Russian Principal Investigator:* **YURI SINYAK, Ph.D.,** Institute of Biomedical Problems	

Inflight Radiation Measurements

U.S. Principal Investigator: **GAUTAM D. BADHWAR, Ph.D.,** NASA/Johnson Space Center

Russian Principal Investigator: **V. M. PETROV,** Institute of Biomedical Problems

Co-Investigators: W. Atwell, B. Cash, E.V. Benton, Yu. A. Akatov, I.V. Tchernykh, V.A. Arkhangelsky, and V.V. Kushin

Technical Assistants: S. Johnson, T. Conroy, R. Dunn, Fadi Riman, and Omar Baltaji

(Mir 18 Final Science Report)

INTRODUCTION

THE HEALTH RISK from radiation exposure of astronauts is a major issue of long term space flights. Sufficient radiation to almost any portion of the body increases the incidence of cancer, particularly myelocytic leukemia. Energetic heavy ions are very effective at causing biological damage, such as cell killing, mutation, neoplastic transformation, and cancer. The two main components of this radiation, trapped particles in the South Atlantic Anomaly (SAA), and galactic cosmic radiation (GCR), are modified in a very complex way as they pass throughout the spacecraft materials and body tissue. The modified radiation field has a significantly different effect on tissue than the primary radiation. Until recently, Russian studies on Mir have focused primarily on absorbed dose and not the biologically important dose equivalent. The dose equivalent can only be obtained by measurements of the full linear energy transfer (LET) spectrum. Estimates of genetic risk require not only the total absorbed dose, but dose rate, and LET. This is because the rate of induction of chromosome aberrations or gene mutations is quite sensitive to these variables.

Objectives

Correlate independent simultaneous space radiation exposure measurements and independent radiation exposure calculations made by NASA/JSC (US) with those made RSA/IBMP (Russia).

Compare the absorbed dose measured throughout the Mir core module with calculated values and determine empirical correction factors for the currently used free space environment models.

Compare the measured linear energy transfer spectra for the GCR and trapped particles with calculated spectra using the most current radiation environment and transport models.

Hypothesis

Current NASA model of trapped radiation requires significant modifications;

Radiation quality factor is significantly modified by the spacecraft shielding mass; and

Is different from that determined by chromosome aberrations in astronaut blood.

Background/History

Measurements of the radiation absorbed dose has been an integral part of all manned space programs. The radiation risk, however, takes in to account the type of radiation and is expressed in terms of dose equivalent. Dose equivalent is a complex function of the energy transfer to tissue and as such depends on both the type and energy of charged particles. Until fairly recently this was calculated using existing free space environment models, knowledge of the spacecraft shielding distribution, and radiation transport models. Thus, uncertainties in any or all of these, led to error in the calculated radiation risk to astronauts. In the current investigation, direct measurements of LET spectra allow us to get the dose equivalent.

METHODS/SCIENCE OPERATIONS

Functional Objectives

FO1. Data downloads through the MIPS system

FO2. Acquire knowledge of Mir shielding mass distribution function

Hardware Items

HW1. ^{254}Cf neutron and ^{137}Cs gamma ray source for detector calibration

HW2. Themolumiscent dosimeters of various kind

HW3. Plastic nuclear track detectors

HW4. Harshaw Model 2000-A Thermoluminesce Detector

HW5. Harshaw 2000-B Automatic Integration Picoemeter

HW6. Tissue Equivalent Proportional Counter

HW7. MIPS computer system with removable hard disk for data download

HW8. Various IBM compatible computers.

RESULTS

List of Pre-, In-, and Postflight Anomalies

Preflight Anomalies

MIPS computer system was never available for software check out and verification, and as a result the file transfer system from hard disk to optical disk was labor intensive.

Inflight Anomalies

TEPC was turned off a number of times without any explanation or consultation with the ground. This resulted in loss of data. Although not critical at this juncture, it would be a potential problem if it were occur during a solar particle event. Some of the passive radiation detectors (PRDs) were not deployed at the agreed upon locations. TEPC memory was not erased after the June 13 download, resulting in the loss of critical data during the STS-71 docking.

Postflight Anomalies

A pair of PRDs from this mission was found on November 16, 1995 and brought back on STS-74. Still missing are two of the three crew dosimeters (the ones worn by Russian cosmonauts). By accounts of the Mir 18 crew these were returned on STS-71 in the suit liners. Thus no intercomparison of crew dosimeters and many of the PRDs is possible. TEPC clock is off by about 15 minutes. No clear explanation of this difference is known.

Completeness/Quality of Data

The quality of data is very good. However data from missing and lost dosimeters will cause us to abandon part of this investigation.

Tables, Graphs, Figures Index

Table 1. Data Collection Sessions/Functional Objectives

Table 2. Comparison of measured and calculated absorbed dose rates.

Figure 1. US and Russian measured dose rate in the core module.

Figure 2. Dose rate as a function of time.

Figure 3. Comparison of the daily dose rate from the R-16 ion chambers and US TEPC.

Figure 4. TEPC measured GCR dose rate versus time.

Figure 5. Measured integral LET spectrum and its comparison with model calculations.

Figure 6. Trapped particles dose rate with time.

Figure 7. TEPC measured differential LET spectrum and its comparison with model calculations.

Figure 8. Comparison of the total (GCR plus trapped) integral LET spectrum measured with TEPC and plastic nuclear track detectors.

Figure 9. Calculated dose and dose equivalent as a function of altitude. The curves are normalized to the observed values at 400 km Mir altitude.

DISCUSSION

Status of Data Analysis

All of the available data from various detectors and groups has been analyzed.

Research Findings

Table 2 gives the results of US PRDs deployed in the Mir core module. The results show that there is a variation of nearly two in absorbed dose throughout the core volume. The location identified as the Commander's cabin has the highest absorbed dose. Shielding distribution functions at the location of these dosimeters were calculated and confirmed that most of the variation in absorbed dose could be explained by shielding mass differences. However, a detailed comparison of the calculated dose rates using these distributions and the AP8 Min trapped proton model, show that there remains significant discrepancies. The model calculations are typically nearly a factor of two higher. There is also reason to believe that the mass shielding distribution functions are not accurate. This has arisen due to not being really sure of the final deployed locations of these dosimeters and not taking in to account other Mir modules (Kvant, Specter).

Figure 1 is a schematic of the Mir core module showing the location of the deployed dosimeters, TEPC, and area passive dosimeter (APD). The numbers in ellipses are the measured dose rate. The letter designation U and R are for US and Russian measurements respectively. The crew dose rate measurements from Russia are based on all three crewmembers but the US dose rate is based on only one crewmember. There are significant differences between the two sets, suggesting that the dosimeters were not mounted at the same shielding location.

Figure 2 shows the absorbed dose rate as measured by TEPC as a function of time. The peak dose rate is nearly 10 μGy/minute. Figure 3 shows a comparison of this rate with that measured by the Russian operational dosimeters,

called R-16. There are two such ions chambers that differ only in the thickness of the aluminum shielding (0.5 and 3.5 g/cm^2) around them, and are meant to provide estimates of the skin and blood forming organ dose rates. The R-16 data are quantized in units of 50 μGy/day. R-16 is located in a less (average of about ~ 4 g/cm^2) shielded location than TEPC. Thus the more heavily shielded R-16 will give data comparable to the TEPC data. This is indeed the case. The TEPC data were separated into two components, GCR and trapped. Figure 4 shows the GCR dose rate as a function of time. The solid curve is the value of the deceleration potential, ϕ, in mV, obtained from the Climax neutron monitor rate and the knowledge of interplanetary magnetic field polarity. The deceleration potential is a measure of changes in the GCR spectra due to solar modulation. Figure 5 is comparison of the measured GCR LET spectrum for the whole flight with model calculations. The model calculations were done using the Badhwar and O'Neill (1993) GCR model of the free space environment and the HZETRN (Cucinotta et al., 1994) radiation transport model. There is good agreement between the two which shows that the calculated and measured radiation quality factors are relatively the same. Further improvements would require that account be taken of the albedo proton and neutrons, spacecraft secondary neutron, and ^{137}Cs source on board the Mir station. Recent measurements of cross-section at GSI machine (Darmstadt, Germany) have indicated that some of the cross-sections used in the HZETRN are incorrect. This will affect the calculated GCR spectrum in the 15-50 keV/μm. The HZETRN code is currently being modified by NASA Langely Research Center to correct for these new cross-sections. Mission integrated GCR dose rate was 153.8 μGy/day, dose equivalent rate of 498.4 mrad/day, and average quality factor of 3.24 (using the ICRP-26 definition of quality factor as a function of LET).

Figure 6 shows the absorbed dose rate due trapped particles as a function of time. Because the trapped particles dip down in to the atmosphere, this radiation is affected by atmospheric heating caused by the solar UV. The solar UV intensity has 27.2 days periodicity (due to solar rotation) and is strongly correlated with the solar radio noise in the 10.7 cm wavelength. The plot shows that even at a fixed shielding location, the dose rate varies by a factor of nearly 2 with time. Part of this variation is certainly due to variation in the exospheric temperature. There are clear indications that sudden changes in the magnetic field bring electrons in to the Mir orbit and produce addition dose rate. Mir orbital station flies in a near fixed attitude. Any changes in this attitude also cause changes in the dose rate due to the fact that the trapped particles have a very sharp pitch angle (angle between the particle velocity vector and local magnetic field vector) distribution. Understanding of this behavior over long time is needed to develop appropriate models of radiation belts. Figure 7 shows the trapped particle LET spectra and its comparison with model calculations. The model calculations were done using the AP8 Min free space model and BRYNTRN radiation transport code. The agreement is poor below LET of 5 keV/μm, the region of almost all of the primary particles. The absorbed dose rate was 145.5 μGy/day, dose equivalent rate of 282.5 μSv/day, and average quality factor of 1.94. This quality factor is larger than model calculations. There are three reasons for this: (i) errors in the AP8 trapped belt model, (ii) neutrons produced by interaction of trapped protons with spacecraft material, and albedo neutrons that are detected by TEPC but not included in the model calculations, and (iii) errors in transport code, particularly the target fragmentation products.

The combined GCR plus trapped proton absorbed dose rate was 299.3 μGy/day, dose equivalent rate was 781 μSv/day, and average quality factor of 2.61. TLDs mounted next to the TEPC measured a total dose rate of 241 μGy/day. TLDs are inefficient in detecting particles with LET > 10 keV/μm and also do not detect neutrons. Using PNTDs we estimate the dose contribution of > 10 keV/μm particles as 31 μGy/day for a total absorbed dose rate of 272 μGy/day from passive detectors. This is only 9% lower than the TEPC measured dose rate and can be explained by the neutron contribution. Figure 8 shows a comparison of the TEPC LET spectrum with that measured by CR-39 PNTDs. The PNTDs have lower LET threshold of 5 keV/μm and are not fully efficient till about 15 keV/μm. In the region of 15-1000 keV/μm the agreement between the two detectors is excellent. These measurements also show that TLDs measured 20% less absorbed dose due their inefficiency for high LET particles and neutrons. If the crew exposures that were measured with TLDs, are corrected for this inefficiency, the US crew skin exposure, amounts to a dose rate of 1130 μSv/day.

The higher measured quality factor means higher biological dose equivalent rate. Figure 9 plots the calculated blood forming organ dose equivalent rate as function of Mir altitude. The projected altitude range for the ISS is expected to be in the region of 370 to 470 km. The exact altitude will depend on solar activity, among other factors. The calculations were made using the best computational male (female) anatomical model, such that the skin dose at 400 km, corresponds to the actual measurements of the US crewmember. The higher dose rates at higher altitude are the direct results of the altitude dependence of the trapped particle fluxes being higher. Based on this analysis, a 35 year female can stay in ISS orbit for about 3 years without violating the proposed new career limits. This will be case if there no other exposures, such as those arising from EVAs or solar energetic particle events.

Conclusion

This investigation has provided detailed information of the radiation field inside the Mir core during the time the current solar minimum. The results show:

Our understanding of the GCR environment is fairly good in predicting the absorbed dose and dose equivalent. However additional work is needed in the area of radiation transport models to better predict the LET spectrum;

The AP8 Min model does not predict the absorbed dose, dose equivalent, or LET spectrum of trapped particles very well. This will introduce significant uncertainties in predicting the crew exposure in future. It is recommended that steps be taken to improve the trapped belt models.

The average radiation quality factor, Q(L), using the ICRP-26 relationship between Q and LET, L, is 2.6. This is higher than model calculations. The major cause of the difference is due to errors in the AP8 Min model. The effect of secondary neutrons that the TEPC measures but are not included in model calculations is also a contributing factor;

Studies of the chromosome aberration in the blood of crewmembers of this flight (Yang et al., 1995) gave a dose equivalent rate of 1260 μSv/day, compared to the skin dose equivalent from physical dosimetry measured rate of 1130 μSv/day. This is a remarkably close agreement.

If the only radiation received by a crewmember is natural (GCR plus trapped particles) inside the spacecraft, crewmembers can stay in orbit for up to three years without exceeding their career limits.

There is a clear need to improve the trapped proton belt models. These static models are completely inadequate for the predicting exposure for long term stay in low Earth orbit.

TABLE 1. DATA COLLECTION SESSIONS/FUNCTIONAL OBJECTIVES

Mission	Scheduled Day	Actual Day	Actual Date	Actual Subjects	Samples/ Parameter
Passive Dosimetry					
STS-71	FD7	FD7	3 Jul 96	N/A	Retrieve dosimeters
STS-71	R+0	R+0	8 Jul 96	N/A	Return of dosimeters for processing.
Crew Dosimetry					
Mir 18	Mar SoyuzLaunch	Mar SoyuzLaunch	Dosimeter Deploy	All Mir 18	US and Russian crew
STS-71	FD7	FD7	3 Jul 96 dosimeter transfer	All Mir 18	US and Russian Crew
STS-71	R+0	Pending	Pending processing	5 of 6 dosimeters	Return Dosimeters
Active Dosimetry (TEPC)					
Mir 18		FD9	24 Mar 96	N/A	TEPC Download
Mir 18	FD20	FD23	4 Apr 96	N/A	TEPC Download
Mir 18	FD34	FD34	18 Apr 96	N/A	TEPC Download
Mir 18	FD48	FD48	2 May 96	N/A	TEPC Download
Mir 18	FD63	FD62	16 May 96	N/A	TEPC Download
Mir 18	FD76	FD77	31 May 96	N/A	TEPC Download/erase
Mir 18	FD90	FD90	13 Jun 96	N/A	TEPC Download
Mir 18	N/A	FD99	26 Jun 96	N/A	TEPC Download
STS-71	FD5	Canceled	Canceled	N/A	TEPC Download

Sessions: Download Linear Energy Transfer Spectra as a function of time

TABLE 2. COMPARISON OF MEASURED AND CALCULATED ABSORBED DOSE RATES

Detector	Location	Detector Shielding (g/cm2)	Measured (US) Dose Rate (mGy/day)	Measured (Russian) Dose Rate (mGy/day)	Calculated Dose Rate* (mGy/day)
PRD 1	Commander cabin	0.16	464.1	488	1091.5
PRD 2	Near TEPC/ Russian Panel 224 Outside Flight Engineer's Cabin	0.16	347.2	290	1088.7
PRD 3	Panel 410	0.16	284.5	364	349.7
PRD 4	Transfer module/ Window # 14	0.16	416.2	451	370.2
PRD 5	Central Control Desk Overhead Panel 307	0.16	283.1	352	569
PRD 6	Behind Panel 325	0.16	428.5	480	
R-16		0.5	-	593	774.8
R-16		3.5	-	225	535.1
TEPC		1.4	299.3	-	349.2
APD	Next to TEPC	0.7	265.9	265	359

* One-half of the AP8 MIN trapped proton model with Daly and Evans /5/ interpolation using the combined detector and shielding probability density (e.g. figure 1) plus the GCR dose rate measured by TEPC (Table 4)

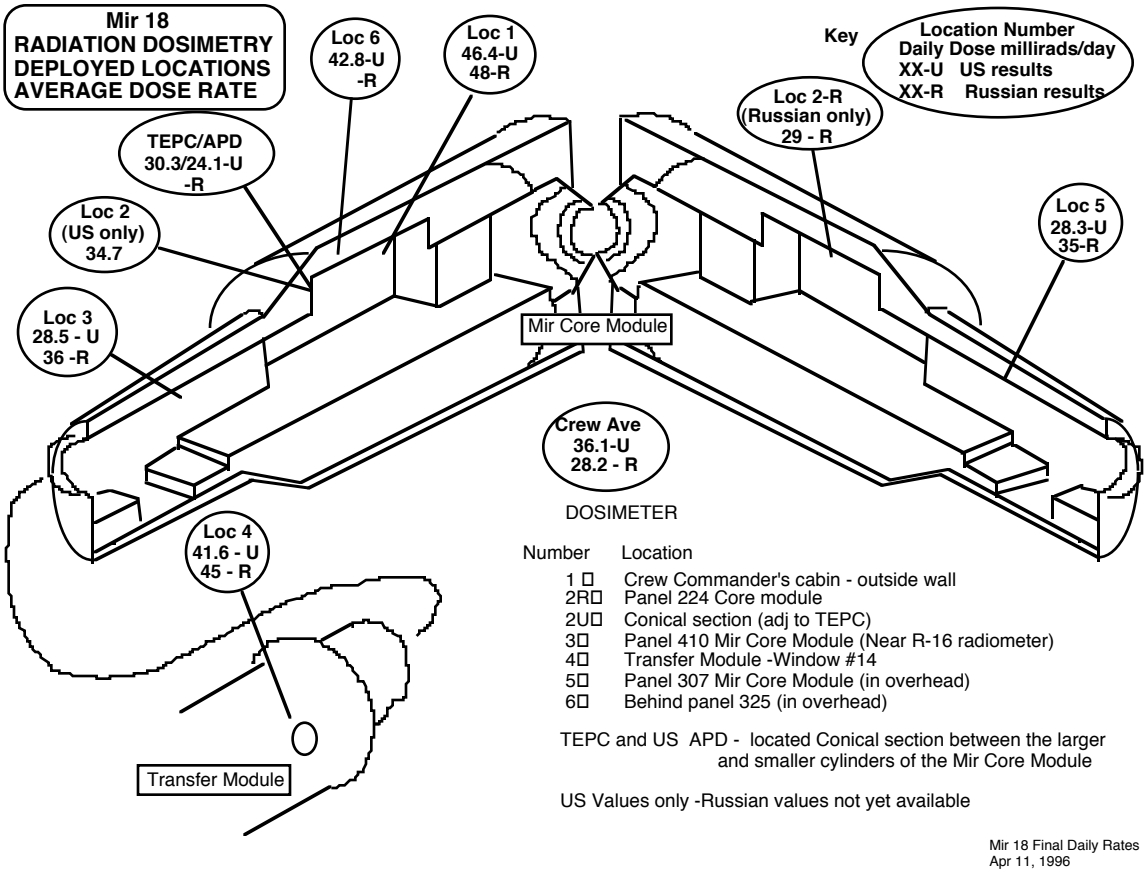

Figure 1. US and Russian measured dose rate in the core module.

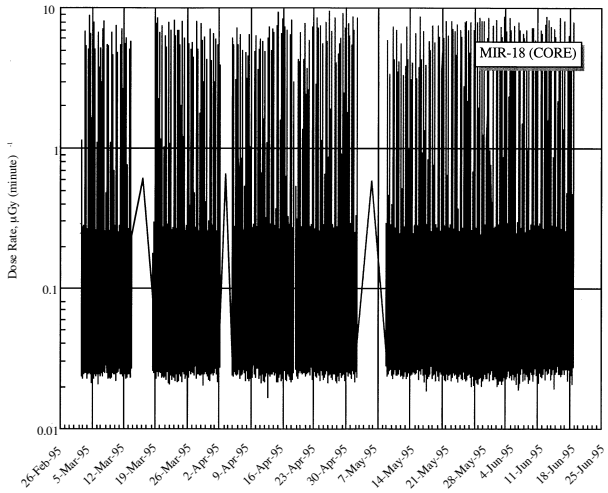

Figure 2. Dose rate as a function of time.

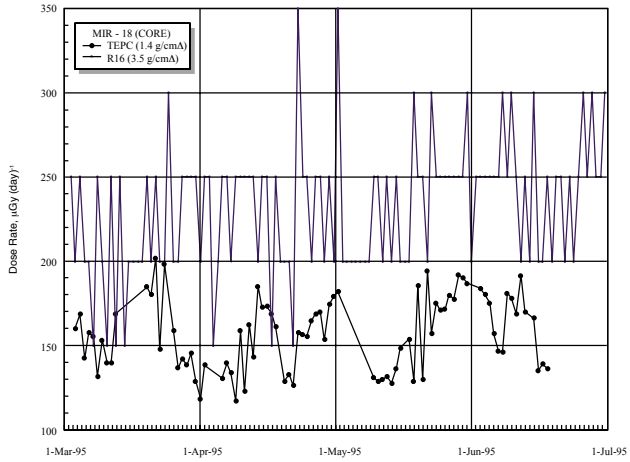

Figure 3. Comparison of the daily dose rate from the R-16 ion chambers and US TEPC.

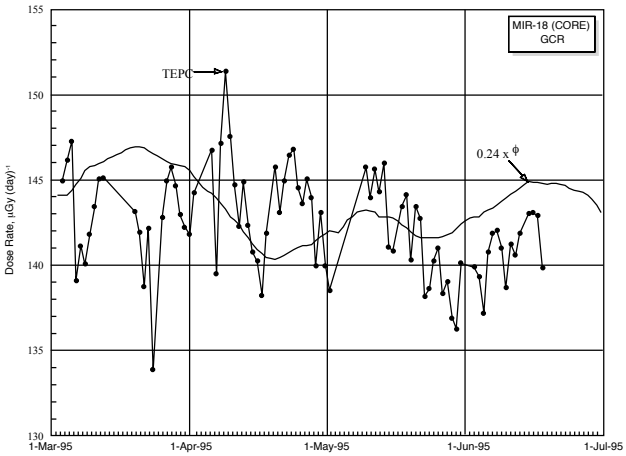

Figure 4. TEPC measured GCR dose rate versus time.

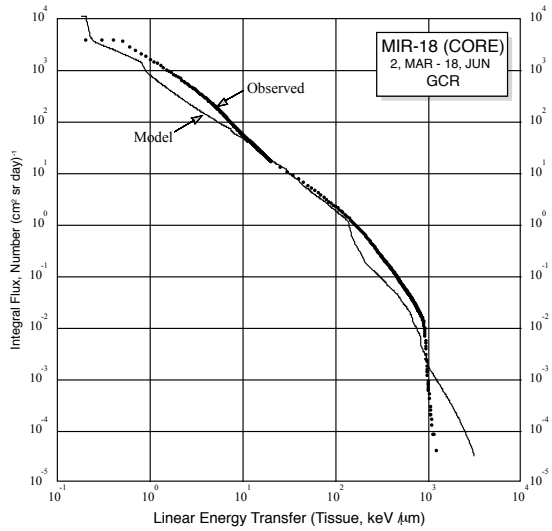

Figure 5. Measured integral LET spectrum and its comparison with model calculations.

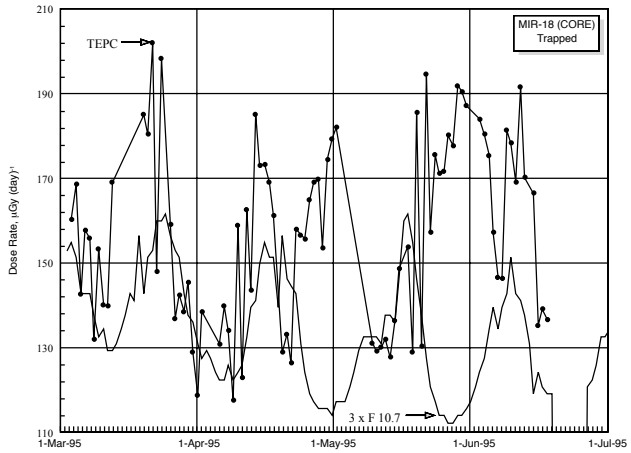

Figure 6. Trapped particles dose rate with time.

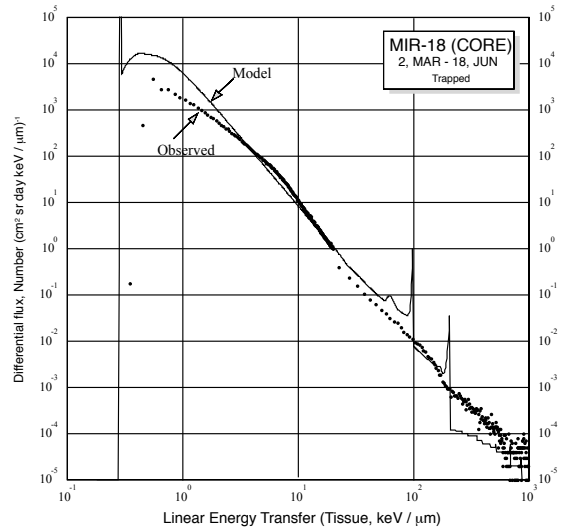

Figure 7. TEPC measured differential LET spectrum and its comparison with model calculations.

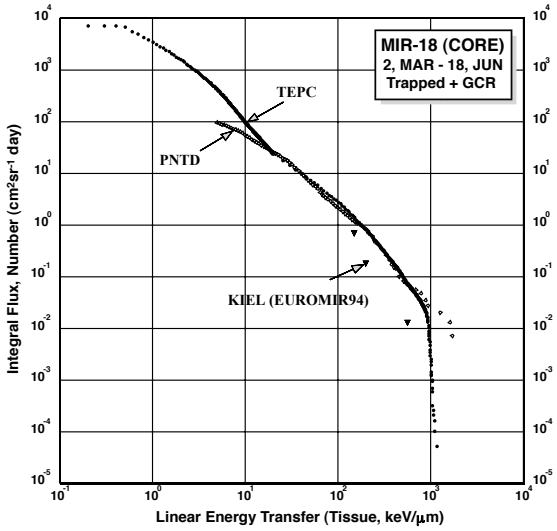

Figure 8. Comparison of the total (GCR plus trapped) integral LET spectrum measured with TEPC and plastic nuclear track detectors.

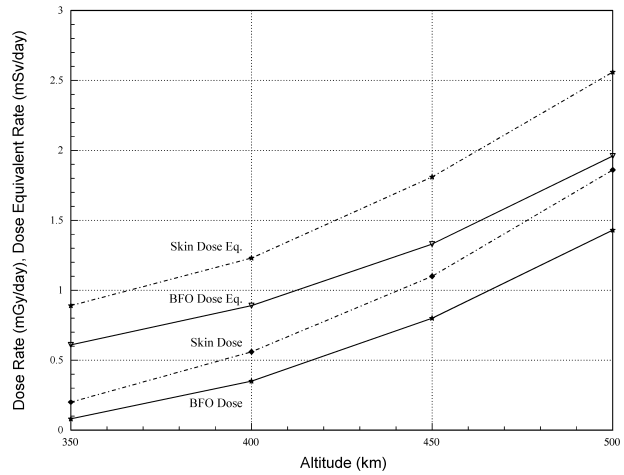

Figure 9. Calculated dose and dose equivalent as a function of altitude. The curves are normalized to the observed values at 400 km Mir altitude.